Heat capacity near the smectic-*A*–hexatic-*B* and hexatic-*B*–*E* transitions of *n*-hexyl-4′-*n*-pentyloxybiphenyl-4-carboxylate (65OBC)

J. M. Viner, D. Lamey, and C. C. Huang
School of Physics and Astronomy, University of Minnesota, Minneapolis, Minnesota 55455

R. Pindak and J. W. Goodby
Bell Laboratories, Murray Hill, New Jersey 07974

(Received 29 November 1982; revised manuscript received 31 May 1983)

High-resolution ac calorimetry was used to measure the heat capacity of *n*-hexyl-4′-*n*-pentyloxybiphenyl-4-carboxylate in the vicinity of the smectic-*A* (Sm*A*)–hexatic-*B* and hexatic-*B*–*E* transitions. The Sm*A*–hexatic-*B* transition was found to be continuous with critical exponents $\alpha^- = \alpha^+ = 0.61 \pm 0.02$ and amplitude ratio $A^+/A^- = 0.84 \pm 0.03$. The addition of a crystalline-*B* material [N-(4-*n*-butyloxybenzylidene)-4′-octylaniline (4O.8), 10 wt. %] produced a weakly-first-order Sm*A*–hexatic-*B* phase transition. The data with $|T - T_c| \geq 100$ mK can be fitted by a power law with $\alpha = 0.49 \pm 0.02$ and $A^+/A^- = 0.82 \pm 0.03$. The large values for the critical exponents and the theoretical suggestion that the Sm *A*–hexatic-*B* transition may be near tricritical point ($\alpha_t = 0.5$) are discussed. The hexatic-*B*–*E* transition was found to be first order in nature.

I. INTRODUCTION

Among the various mesophases found in liquid crystals, the structural characterization of the smectic phases with in-plane order has been the least complete. One such smectic phase, the *B* phase, was known to consist of molecules hexagonally ordered within each layer with the molecules oriented perpendicular to the layer planes;[1,2] but, for some time, the unanswered question had been to what extent the order was local or long-range in nature. X-ray studies have recently shown that the *B* phase can actually be of two microscopically distinct forms: the crystalline-*B* phase and the hexatic-*B* phase. The crystalline-*B* phase has three-dimensional (3D) crystalline order as shown by x-ray studies[3–5] Various packing arrangements between layers are possible. For example, the liquid crystal N-(4-*n*-butyloxybenzylidene)-4′-*n*-octylaniline (4O.8) has a crystalline phase consisting of hexagonal sheets stacked in an *ABAB* sequence with 3D long-range order.[4] Hints of another type of *B* phase came with reports of a *B* phase without long-range interlayer correlations.[6] A theoretical model for this phase was proposed by Birgeneau and Litster,[7] building upon the two-dimensional (2D) melting theory of Halperin and Nelson.[8] Halperin and Nelson claimed that a 2D crystal could melt into an intermediate hexatic phase lacking positional correlations but exhibiting bond-orientational order. Birgeneau and Litster proposed a 3D liquid-crystal phase consisting of stacked hexatic layers. In search of such a phase, Goodby[9] synthesized the liquid crystal *n*-hexyl-4′-*n*-pentyloxybiphenyl-4-carboxylate (65OBC) which has the following sequence of phases on cooling: isotropic (*I*), smectic-*A* (Sm*A*), *B* phase, *E* phase, and

$$I \overset{84^\circ}{\text{——}} \text{Sm}A \overset{67^\circ}{\text{——}} B \overset{61^\circ}{\text{——}} E$$

with the melting point at 65 °C. Using x-ray techniques on free-standing liquid-crystal films, Pindak *et al.*[10] have found that the *B* phase of 65OBC, now called the hexatic-*B* phase, has short-range in-plane positional correlations and long-range 3D sixfold bond-orientational order. Short-range herringbone packing order[11] was also found in the hexatic-*B* phase. The *E* phase is characterized by long-range positional, bond-orientational, and herringbone order.

A series of experiments then followed which determined the nature of the phase transitions in 65OBC, particularly the Sm*A*–hexatic-*B* transition. Huang *et al.*,[12] using heat-capacity measurements, have shown the Sm*A*–hexactic-*B* transtition to be continuous with a power-law divergence fit that gave $\alpha = 0.64 \pm 0.04$. (4O.8 had a first-order Sm*A*–crystalline-*B* transition.) Mechanical measurements[13] on free-standing films demonstrated the absence of an in-plane shear modulus for 65OBC in the hexatic-*B* phase consistent with short-range in-plane correlations from x-ray measurements.[11] (4O.8 gave a solid-like shear modulus in the crystalline-*B* phase.[14]) Assuming that the nematic order parameter S and bond-orientational order parameter ψ are coupled, then an increase in $\langle \psi^* \psi \rangle$ or $\langle \psi \rangle$ will enhance S and thus the birefringence Δn should increase. Rosenblatt and Ho,[15] using the above idea, found $\alpha = 0.60 \pm 0.05$ consistent with heat-capacity measurements and $\beta = 0.19 \pm 0.03$, the critical exponent of ψ, from the anomalous part $\delta(\Delta n)$ of the birefringence below the Sm*A*–hexatic-*B* transition of 65OBC.

Because x-ray results indicated that herringbone pack-

ing order exists in 65OBC, Bruinsma and Aeppli[16] have recently proposed a theory based on the coupling of bond-orientational order with herringbone order to explain the nature of the SmA—hexatic-B transition. The theory suggests that the SmA—hexatic-B transition of 65OBC may be near a herringbone-fluctuation-induced tricritical point.

The remainder of the paper consists of three sections. Section II presents a detailed description of the ac calorimeter system and experimental procedure for measuring liquid-crystal heat capacity. Section III considers the heat capacity of 65OBC in the temperature range 59—76 °C which includes the SmA—hexatic-B and hexatic-B—E phase transitions. The heat-capacity anomaly of the SmA—hexatic-B transition for a 40.8-65OBC 10-90% mixture system follows. Details of the data analysis are also given. Finally, the natures of the above two transitions are discussed in Sec. IV.

II. EXPERIMENTAL METHOD

The quasiadiabatic ac calorimetric technique of Sullivan and Seidel[17] was used to measure the variation of liquid-crystal heat capacity with temperature.[18–20] A periodic heat input of constant amplitude ΔQ causes a periodic temperature oscillation in the liquid crystal. The heat capacity C is inversely proportional to the temperature-oscillation amplitude ΔT.

The ac calorimetric technique permits the use of ac amplification and phase-lock detection with a resulting high sensitivity and low noise. Reduced temperature, impurity, and inhomogeneity gradients result from the use of a small sample size. In addition, the method allows for a continuous measurement of heat capacity as a function of temperature.

Figure 1(a) shows schematically a liquid-crystal sample of thickness h as used in the ac calorimeter. Of the heat energy ΔQ applied to region X, a part ΔQ_1 is dissipated with a time constant τ_1 primarily through an exchange gas to the heat reservoir and another part ΔQ_2 goes to region Y with a time constant τ_2. The heat capacity C is inversely proportional to the resulting temperature-oscillation amplitude ΔT in region Y. Sullivan and Seidel[17] have shown for one-dimensional heat flow that

$$\Delta T=\frac{\Delta P_A}{\omega C_A}\left[1+\frac{1}{(\omega\tau_1)^2}+(\omega\tau_2)^2+2(10)^{1/2}\frac{\tau_2}{\tau_1}\right]^{-1/2}, \tag{2.1}$$

where ΔP_A is the power-oscillation amplitude per unit area applied to region X, ω is the angular frequency of oscillation, C_A is the heat capacity per unit area, $\tau_2=h^2/[3(10)^{1/2}n]$, n is the thermal diffusivity of the sample, and $\tau_1=C/g$ with g the sample-to-reservoir thermal conductance. For operation independent of the time constants τ_1 and τ_2, then

$$\omega\tau_1\gg 1,\quad \omega\tau_2\ll 1\ . \tag{2.2}$$

Here, $\omega\tau_1\gg 1$ ensures negligible heat loss to the heat reservoir over one oscillation cycle (quasiadiabatic condition) and $\omega\tau_2\ll 1$ ensures sample thermal equilibrium. τ_1 may be adjusted by changing g; τ_2 by changing h.

Because liquid crystals have a small thermal conductivity κ_L ($\kappa_L\simeq 0.1\kappa_{\text{glass}}$), the sample must be thin to obtain a measurable ΔT in region Y. In addition to guaranteeing $\omega\tau_2\ll 1$, a sample thin enough gives $h\ll L_0$, where L_0 is the thermal diffusion length. To eliminate finite-size effects, the correlation length ξ associated with a particular phase transition must satisfy $\xi\ll h$.

The experimental apparatus consists of a sample cell containing the liquid crystal, an oven to control the average sample temperature, and associated electronics. Figure 1(b) shows the sample cell with liquid crystal L, glass slides G, ac heater H, ac thermocouple A, and dc thermocouple D.

Two cover glass slides G form the liquid-crystal container. Each slide is masked and then etched in a hydrofluoric-acid—distilled-water solution. The etching solution thins the glass in the unmasked regions to form depressions, one of which holds the liquid crystal. The thinning process also reduces addendum heat capacity from the glass slides. Before an experiment the etched glass slides are cleaned in an acidic solution. For 65OBC the depression containing the liquid crystal was 20 μm deep by 1.0 cm in diameter with 25-μm-thick glass above and below. Consider the power-law representation for the correlation length in the critical region $\xi=\xi_0|t|^{-\nu}$, where $t=(T-T_c)/T_c$. Assuming $\xi_0\simeq 30$ Å, one molecular length, then $\xi<h$ ($\xi\lesssim 1$ μm, $h=20$ μm) for $|t|\gtrsim 10^{-5}$. The glass slides contributed 74% to the total measured background heat capacity at T_c.

On the bottom surface of the lower glass slide a gold

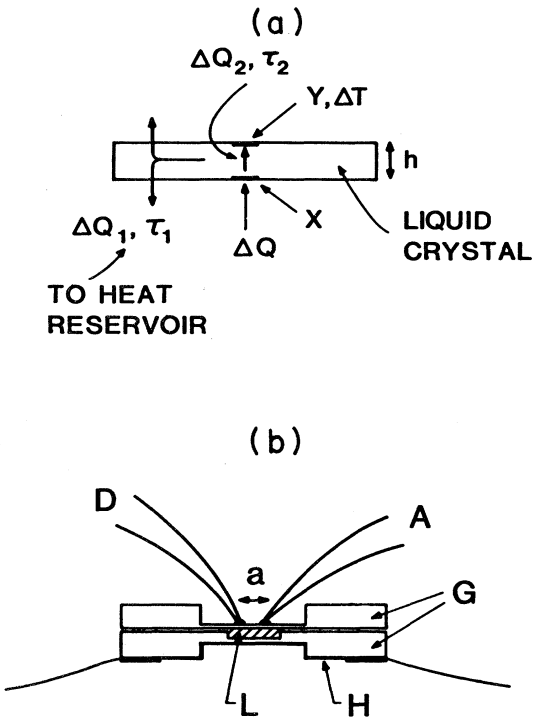

FIG. 1. (a) Simplified liquid-crystal sample cross section. (b) Liquid-crystal sample-cell cross section.

thin-film heater H provides the periodic (ac) heat ΔQ. A gold film thickness of 90 Å over an area of 2.0 cm^2 gives a heater with a resistance R of 50 Ω and negligible addendum heat capacity. To minimize ac-heater power fluctuations δP due to resistance fluctuations δR in R, the heater resistance is matched as closely as possible to the output resistance ($R_0=50$ Ω) of the sine-wave oscillator which drives the heater. For 65OBC, $R=72$ Ω and $\delta R=0.6$ Ω during an experiment, which means that $\delta P\simeq 1.5$ μW for an input power $P=1$ mW, a 0.15% power variation.

Thermocouple A senses the sample temperature-oscillation amplitude ΔT within a distance of approximately one thermal diffusion length L_0. Thermocouple D measures the average (dc) sample temperature. Both thermocouples A and D are made from 25-μm-diam chromel and constantan wires, spot welded and flattened to 5 μm at the thermocouple junction. A flattened side of each thermocouple is attached to the upper half of the top glass slide with a small amount of GE 7031 varnish. A flattened junction improves thermal contact between the thermocouple junction and the glass slide. A and D are electrically isolated and spaced a distance a apart. D lies close to A to measure the average temperature at A, but not so close as to contribute to the heat capacity measured by A ($a\simeq 4L_0$). For 65OBC thermocouple A and the GE 7031 varnish adhesive gave an addendum heat-capacity contribution of 17% to the total measured background heat capacity.

An oven which controls the sample-cell average temperature consists primarily of a heat reservoir and a sample-cell—heat-reservoir thermal link. A noninductive resistive heater heats an aluminum block to form the heat reservoir. Thermal compound secures the sample cell to an anodized aluminum base in the aluminum block and a copper disc holds the sample cell in place against the aluminum base. Argon exchange gas normally at a pressure of 0.5 atm contributes 60% to the sample-to-reservoir thermal conductance g; the anodized aluminum base 40% to g. For the 65OBC sample, $g=5\times 10^{-3}$ W/K and the sample-to-bath time constant $\tau_1=4$ sec.

Figure 2 shows the electronic apparatus used for measuring the liquid-crystal heat capacity C as a function of temperature T. A sine-wave oscillator with an output resistance of 50 Ω provides the ac-heater power and the lock-in amplifier reference signal. Thermocouple A with a resistance of 15 Ω senses the resulting ac temperature oscillations of amplitude ΔT. A Princeton Applied Research (PAR) 190 transformer (1:100 turn ratio) helps to match the low thermocouple resistance to the lock-in

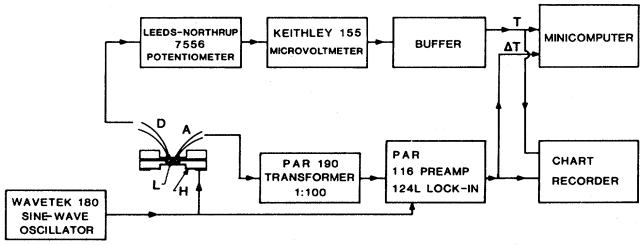

FIG. 2. Electronics for measuring T and ΔT of a liquid-crystal sample.

amplifier high input resistance thereby improving the system signal-to-noise ratio. The thermocouple-A—transformer primary circuit limits the low-frequency response to 0.2 Hz. A 4-mK zero-to-peak (0-p) temperature-oscillation amplitude gives a lock-in amplifier signal of, typically, 20 μV rms with 0.05-μV peak-to-peak noise.

Thermocouple D with a resistance of 50 Ω measures the average (dc) sample temperature T. A Leeds and Northrup 7556 potentiometer and a Keithly 155 microvoltmeter null detector read the dc thermocouple potential. The ac and dc thermocouple signals are recorded on a chart recorder. A minicomputer reads and averages the temperature signals and then outputs the dc temperature in degrees Celsius along with the corresponding total relative heat capacity (0.1% resolution).

When initially placing a liquid-crystal sample inside the oven, the following precautions are taken to reduce sample deterioration. At room temperature an excess amount of liquid crystal is placed in the upper depression L of the lower glass slide. The top glass slide then covers the liquid crystal. A thin copper disc loosely clamps the two slides against an anodized aluminum base inside the oven. The oven is then sealed and evacuated overnight at a temperature just below the liquid-crystal melting temperature. A vacuum prevents the formation of air bubbles in the liquid crystal after melting the sample and an elevated temperature facilitates outgassing. The temperature is then raised until the liquid crystal reaches the isotropic phase which allows excess liquid crystal to leak from the sample cell. After introducing argon gas into the oven, the sample cell is tightly clamped against the aluminum base while the liquid crystal remains in the isotropic phase and argon gas flows through the system. With 0.5 atm of argon gas in the oven to prevent sample deterioration and provide a sample-to-heat reservoir thermal link, leakage of liquid crystal from the sample cell is checked. If leakage occurs, then ΔT gradually increases at constant T. A constant value for ΔT indicates no leakage. The sample is then cooled to an appropriate lower temperature phase for the purpose of measuring the frequency response as described by Eq. (2.1).

To select the proper operating frequency f ($\omega=2\pi f$), a plot of $f\Delta T$ versus f is made in the temperature range of interest. From Eq. (2.1), f is chosen such that τ_1 and τ_2 are unimportant. That is, f is chosen in a region such that $f\Delta T$ has a constant value. Because $\omega\tau_2$ usually increases at a phase transition and $1/f$ noise increases with decreasing frequency, f is selected as large as possible consistent with $\omega\tau_2\ll 1$. For 65OBC at the SmA—hexatic-B transition temperature (67.3 °C) a graph of $f\Delta T$ versus f gave $f_2=1/(2\pi\tau_2)=50$ Hz for a 70-μm-thick sample cell including the ac thermocouple and ac heater. An operating frequency of 1.74 Hz was chosen to satisfy $\omega\tau_2=f/f_2\ll 1$.

To measure heat capacity as a function of temperature the value of ΔT is continuously recorded while slowly sweeping the average (dc) temperature T of the sample. For 65OBC, T changed by 50 mK/min far from the SmA—hexatic-B phase transition ($\Delta T=3.2$ mK 0-p) to 1.4 mK/min near the transition ($\Delta T=1.7$ mK 0-p). The

sweep rate r_s was slow enough that the liquid crystal remained in thermal equilibrium, i.e., $r_s \simeq 50$ mK/min $\ll \omega_2 \Delta T = 5.6 \times 10^4$ mK/min far from the transition and $r_s \simeq 1.4$ mK/min $\ll \omega_2 \Delta T = 3.2 \times 10^4$ mK/ min near the transition.

In summary, a high-resolution ac calorimeter now exists for measuring the heat capacity of liquid crystals to $\pm 0.1\%$ resolution of the total sample-cell heat capacity over the temperature range 10—150 °C. Average temperatures are known to 100-mK absolute accuracy and 2-mK relative accuracy. In addition, the time to perform an experiment is normally about ten hours which means that the system is excellent for exploratory work. The short experimental time also means less sample deterioration and therefore less T_c drift, if T_c drift is present. The sample-cell glass pieces are easily cleaned in an ultrasonic cleaner and a used sample-cell containing liquid crystal may be easily stored for possible future measurements. Finally, the system may easily be adapted to light scattering experiments. However, the ac calorimeter does have the disadvantage of heat-capacity measurements being no better than 10% in accuracy.

III. DATA AND DATA ANALYSIS

Figure 3 shows the total heat capacity per unit area C_p (liquid crystal and sample cell) for 65OBC as a function of temperature T from 59 to 76 °C. An expansion of the temperature axis (Fig. 4) reveals the SmA—hexatic-B phase transition to be approximately symmetric about the temperature $T_p = 67.290$ °C at the heat-capacity peak, which suggests a continuous phase transition. The hexatic-B—E phase transition (Fig. 3) shows a nonsymmetric peak with quite noticeable thermal hysteresis and no pretransitional fluctuations. Thermal hysteresis is indicative of a first-order phase transition.

Because the liquid crystal 4O.8 has a crystalline-B phase with long-range in-plane and interplane positional correlations, whereas 65OBC has a hexatic-B phase with short-range in-plane ($\xi_{\|} \simeq 80$ Å) and interplane ($\xi_{\perp} \simeq 30$ Å) correlations,[10] the addition of 4O.8 to 65OBC may enhance and reveal the function of in-plane and interplane correlations for the SmA—hexatic-B phase transition. For

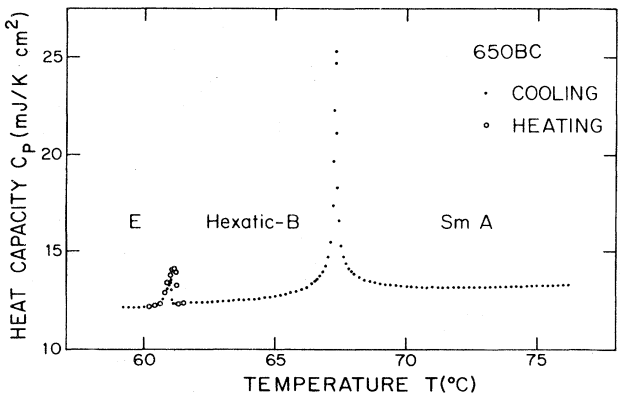

FIG. 3. Total sample-cell heat capacity per unit area of 65OBC as a function of temperature from 59 to 76 °C showing the SmA—hexatic-B and hexatic-B—E transitions.

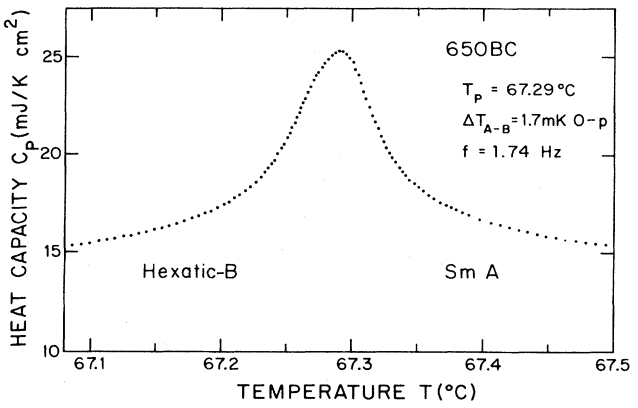

FIG. 4. Total sample-cell heat capacity per unit area of 65OBC near the SmA—hexatic-B transition on an expanded temperature axis (67.1—67.5 °C).

the case of 10% 4O.8 in 65OBC by weight, Fig. 5 shows the relative heat capacity C_p as a function of temperature T. The 65OBC portion of the mixture system came from a high-purity preparation with $T_c = 67.930$ °C for the SmA—hexatic-B transition.[12] The heat-capacity anomaly of the 10-90% mixture system is approximately symmetric about $T_p = 67.310$ °C, but shows a sharper decrease in heat capacity near T_p than does undiluted 65OBC. Increasing the amount of 4O.8 in 65OBC to 30.5% by weight results in a hysteretic heat capacity reminiscent of pure 4O.8.[12] The 30.5-69.5% mixture system exhibits a SmA-B phase transition[9] with first-order behavior.

Because C_p versus T for the SmA—hexatic-B transition displays a C_p divergence characteristic of critical phenomena, the heat-capacity data was fitted to the following equations:

$$C_p^- = A^- |t|^{-\alpha^-} + B^- + D^- t, \quad T < T_c$$
$$C_p^+ = A^+ |t|^{-\alpha^+} + B^+ + D^+ t, \quad T > T_c \tag{3.1}$$

where $t = (T - T_c)/T_c$ and T_c is the transition temperature. The term $A|t|^{-\alpha}$ describes critical behavior, whereas $B + DT$ represents background heat capacity C_B.

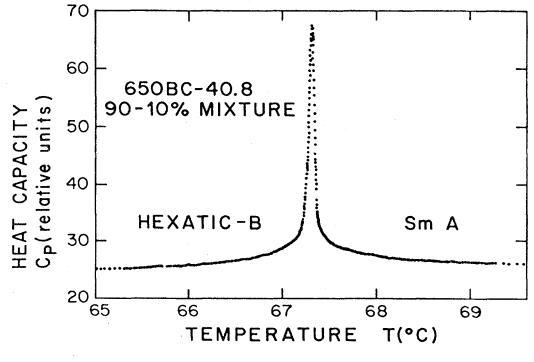

FIG. 5. Total sample-cell heat capacity per unit area of a 4O.8-65OBC 10-90% by weight mixture for the SmA—hexatic-B transition in the temperature range 67.31 ±2.3 °C.

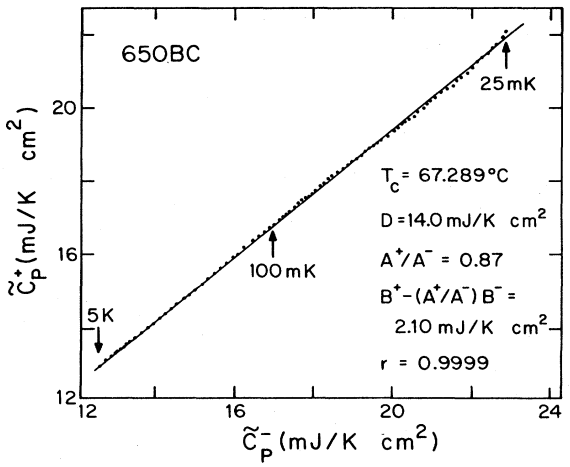

FIG. 6. $\tilde{C}_p^+$ vs $\tilde{C}_p^-$ at equal values of $|t|$ in the temperature range 25 mK $\leq |T-T_c| \leq 5$ K near the SmA–hexatic-B transition of 650BC.

In all the cases the constraint $D^-=D^+=D$ was imposed. In general, the parameters $A^\pm$, $\alpha^\pm$, $B^\pm$, D, and T_c were determined using a least-squares procedure of minimizing the variance s^2 of the fit.[21] The standard deviation σ_i of each data point (T_i,C_{pi}) provided a $1/\sigma_i^2$ weighting to each data point. Fluctuations $\sigma_{C_{pi}}$ in the measured total heat capacity C_{pi} and fluctuations σ_{T_i} in the measured average temperature T_i, assumed independent, were combined and ascribed to C_{pi} only as

$$\sigma_i^2=\sigma_{C_{pi}}^2+\left[\frac{\partial C_p}{\partial T}\right]^2\sigma_{T_i}^2 . \tag{3.2}$$

$\sigma_{C_{pi}}$ was assumed as ηC_{pi} with $\eta\simeq 0.001$ as found from measured fluctuations in C_{pi}. σ_{T_i} was taken as the rms value of the temperature-oscillation amplitude; $\sigma_{T_i}\simeq 2$ mK near the SmA–hexatic-B transition.

Two methods of data analysis were used to determine T_c, D, $\alpha^\pm$, A^+/A^-, B^+, and B^-: the method due to Lederman[22] and a nonlinear least-squares-fitting analysis. In the method due to Lederman, $\tilde{C}_p^\pm$ is defined as

$$\tilde{C}_p^\pm=C_p^\pm-Dt \tag{3.3}$$

and using Eq. (3.1) with t the same magnitude for $t>0$ and $t<0$, then

$$\tilde{C}_p^+=\left[\frac{A^+}{A^-}\right]\tilde{C}_p^-+\left[B^+-\frac{A^+}{A^-}B^-\right] \tag{3.4}$$

assuming that the scaling law $\alpha^-=\alpha^+$ holds. Maximizing the linear correlation coefficient[21] r between $\tilde{C}_p^-$ and $\tilde{C}_p^+$ with respect to T_c, D, and the temperature-fitting range ΔT_r using a least-squares-fitting scheme gave $r=0.9999$ for 650BC in the range 25 mK $\leq |T-T_c| \leq 5$ K with $T_c=67.289$ °C, $D=0.0140$ J/K cm², $A^+/A^-=0.87$, and $B^+-(A^+/A^-)B^-=2.10\times10^{-3}$ J/K cm² (Fig. 6). The remaining unknown parameters α, B^+, and B^- were found by scaling the $\tilde{C}_p^-$ data using Eq. (3.4) and merging the scaled $\tilde{C}_p^-$ with the $\tilde{C}_p^+$ data to form a merged data set (T_i,C_{pm_i}). A linear-least-squares analysis was performed to fit the (T_i,C_{pm_i}) data to $\log_{10}(\Delta C_{pm})$ versus $\log_{10}|t|$, where $\Delta C_{pm}=C_{pm}-Dt-B^+$. Minimizing the variance s^2 of the fit to $\log_{10}(\Delta C_{pm})$ versus $\log_{10}|t|$ with respect to B^+ gave $\alpha=0.60\pm0.02$ and $B^+=0.0126$ J/K cm². From $B^+-(A^+/A^-)B^-$, then $B^-=0.0121$ J/K cm². The results are summarized in Table I.

When applied to the 4O.8-650BC 10-90 % mixture system, the above method would not give a good correlation coefficient r for $|T-T_c|<100$ mK. For a temperature-fitting range 107 mK $\leq |T-T_c| \leq 8.3$ K, then $r=0.9996$, $T_c=67.315$ °C,[12] $D=19.7$, $A^+/A^-=0.82$, and $B^+-(A^+/A^-)B^-=5.28$ in relative units from the linear correlation of $\tilde{C}_p^+$ and $\tilde{C}_p^-$. As with undiluted 650BC, $r=1$ and scaling ($\alpha^-=\alpha^+$) holds for the SmA–hexatic-B transition, but now over a lesser temperature-fitting range. Merging the 10-90 % mixture system data in the manner as described for undiluted 650BC gave $\alpha=0.50$, $B^+=24.3$, and, from $B^+-(A^+/A^-)B^-$, $B^-=23.3$ in relative units. Table II gives a summary of the above results.

The nonlinear least-squares-fitting analysis minimizes the reduced chi square[21] χ_ν^2 simultaneously with respect to the parameters $A^\pm$, $\alpha^\pm$, $B^\pm$, D, and T_c in Eq. (3.1). Letting β_j $(j=1,\ldots,m)$ represent the parameters of $C_p(t)$ and C_{pi} represent the heat capacity of the ith data point of N data points, then a minimum in χ_ν^2 with respect to all β_j requires

$$\sum_{i=1}^{N}\frac{[C_{pi}-C_p(t_i)]}{\sigma_i^2}\left[\frac{\partial C_p(t)}{\partial\beta_j}\right]_{t_i}=0,\quad j=1,\ldots,m . \tag{3.5}$$

Equations (3.5) are solved simultaneously using an algorithm based on a nested Newton-Raphson method.[23] Starting with assumed initial values for α^-, α^+, and T_c, χ_ν^2 is minimized with respect to all other parameters $A^\pm$, $B^\pm$, and D. Then a Newton-Raphson iteration determines new values for α^-, α^+, and T_c. The above process is repeated until the parameter values converge.

TABLE I. Summary of data-fitting results (650BC).

Method of analysis	T_c (°C)	D (J/K cm²)	A^+/A^-	α^-	α^+	B^- (J/K cm²)	B^+ (J/K cm²)
Lederman	67.289	0.0139	0.86	0.60	0.60	0.0121	0.0126
Nonlinear-least-squares fit							
$\alpha^-=\alpha^+$	67.290	0.0126	0.84	0.61	0.61	0.0121	0.0126
$\alpha^-\neq\alpha^+$	67.287	0.0097	0.51	0.58	0.64	0.0120	0.0127

TABLE II. Summary of data-fitting results (65OBC-40.8 90-10 % mixture).

Method of analysis	T_c (°C)	D (Rel.)	A^+/A^-	α^-	α^+	B^- (Rel.)	B^+ (Rel.)
Lederman	67.315	19.7	0.82	0.50	0.50	23.3	24.3
Nonlinear-least-squares fit							
$\alpha^-=\alpha^+$	67.313	19.2	0.82	0.49	0.49	23.2	24.2
$\alpha^-\neq\alpha^+$	67.310	18.1	0.69	0.48	0.50	23.1	24.3

For the nonlinear-least-squares analysis, two cases were considered. Case 1 imposed the constraint of scaling $\alpha^-=\alpha^+$ which gave $\alpha^-=\alpha^+=0.61\pm0.02$, $A^+/A^-=0.84\pm0.03$, and other parameters (Table I) for 25 mK $\leq |T-T_c| \leq 5$ K. A graph of $\log_{10}[\Delta C_p/\Delta C_p(\max)]$ versus $\log_{10}|t|$ for $T<T_c$ and $T>T_c$ under the constraint $\alpha^-=\alpha^+$ is shown in Fig. 7. Case 2 relaxed the α constraint to $\alpha^-\neq\alpha^+$ which gave $\alpha^-=0.58\pm0.02$ and $\alpha^+=0.64\pm0.02$ with $A^+/A^-=0.51\pm0.02$. Although the difference between α^- and α^+ is small, α^+ is higher than α^-. The same behavior was observed in 65OBC sample 1. The reason for the difference between α^- and α^+ is, as yet, unknown.

The SmA—hexatic-B phase transition data for the 65OBC-4O.8, 90-10 % mixture system was also analyzed using the nonlinear-least-squares procedure. Figure 8 shows the result of fitting $\log_{10}[\Delta C_p/\Delta C_p(\max)]$ versus $\log_{10}|t|$ in the temperature range 100 mK $\leq |T-T_c| \leq 8$ K under the scaling constraint $\alpha^-=\alpha^+$. The parameters are given in Table II. The fitting range 100 mK $\leq |T-T_c| \leq 8$ K was chosen for the following reason. When the data were fit in the temperature range $T_n \leq |T-T_c| \leq 8$ K, then α decreased from 0.59 to an asymptotic value of 0.49 and χ^2_ν decreased from 60 to 5.0 as T_n changed from 20 mK to 100 mK. Relaxing the constraint $\alpha^-=\alpha^+$ to $\alpha^-\neq\alpha^+$ gave $\alpha^-=0.48$, $\alpha^+=0.50$, and $A^+/A^-=0.69$ for 100 mK $\leq |T-T_c| \leq 8$ K. Table II presents the other fitting parameters.

The determination of parameter uncertainties is based on the following idea. s will be a function of all parameters, that is, $s=s(A^\pm,\alpha^\pm,B^\pm,D,T_c)$. To determine, for example, the uncertainty σ_{α^+} in α^+, fix all other parameters at values that give $s=s_{\min}$. Subsequently vary α^+ until $s=2s_{\min}$. Then

$$\sigma_{\alpha^+} \equiv |\alpha^+(2s_{\min})-\alpha^+(s_{\min})| \ . \tag{3.6}$$

The parameter uncertainties calculated in the above manner gave uncertainty values of $\sigma_\alpha=0.02$ and $\sigma_{A^+/A^-}=0.03$.

Let ΔT_r be the temperature range $T_n \leq |T-T_c| \leq T_f$ over which the data was fit for $T<T_c$ and $T>T_c$. T_n labels the range limit near T_c and T_f far from T_c. To test the stability of α (under the constraint $\alpha^-=\alpha^+$) or any other parameter of Eq. (3.1), the range ΔT_r was varied in the following two ways. First, T_f was held fixed at 5 K and T_n was varied in the range 20 mK $\leq T_n \leq$ 100 mK which gave an α variation $0.60 \leq \alpha \leq 0.63$. Second, $\Delta T_r' < \Delta T_r$ was chosen and moved over the interval 20 mK $\leq |T-T_c| \leq 5$ K. For $\Delta T_r'=2$ decades in $|T-T_c|$, then α varied in the range $0.58 \leq \alpha \leq 0.62$. Similarly for $\Delta T_r'=1.5$ decades in $|T-T_c|$, α changed as $0.57 \leq \alpha \leq 0.62$. Figure 9 summarizes the above results showing α versus T_n for 20 mK $\leq T_n \leq$ 100 mK. The above results indicate that α remains stable with respect to fitting range.

IV. DISCUSSION

The C_p-versus-T data from Fig. 3 shows the hexatic-B—E transition to be asymmetric with thermal hysteresis. The heat-capacity-peak temperature for heating ($T_{ph}=61.135$ °C) is greater than that for cooling ($T_{pc}=61.030$ °C) by 105 mK. And the heat-capacity-peak

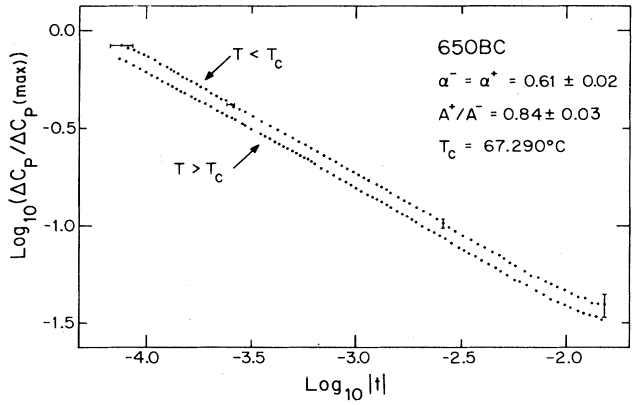

FIG. 7. $\log_{10}[\Delta C_p/\Delta C_p(\max)]$ vs $\log_{10}|t|$ near the SmA—hexatic-B transition of 65OBC, $7.5\times10^{-5} \leq |t| \leq 1.5\times10^{-2}$.

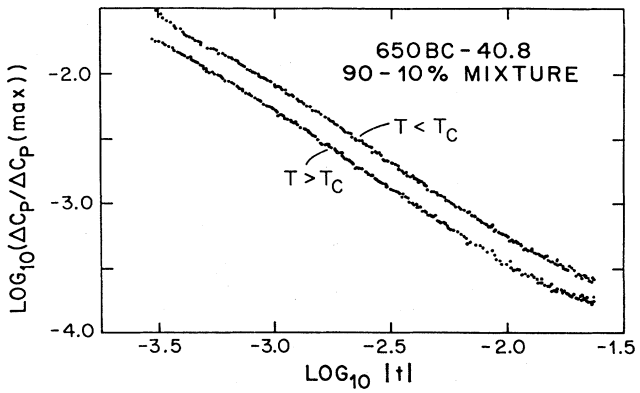

FIG. 8. $\log_{10}[\Delta C_p/\Delta C_p(\max)]$ vs $\log_{10}|t|$ near the SmA—hexatic-B transition of a 4O.8-65OBC 10-90 % mixture system, $2.9\times10^{-4} \leq |t| \leq 2.3\times10^{-2}$.

amplitude for heating exceeds the peak amplitude for cooling by 20%. In addition, the heat-capacity-peak amplitude for heating increases with decreasing time spent in the E phase before warming back into the hexatic-B phase. The differences in transition temperatures and peak heights indicate the presence of superheating and supercooling. The above observations of thermal hysteresis show the hexatic-B–E transition to be first order in nature; no discernible pretransitional anomaly occurs. The hexatic-B–E transition requires the development of both long-range herringbone and long-range in-plane positional ordering. From symmetry arguments a first-order transition is expected[16]; hence, theory and experiment are consistent.

The SmA–hexatic-B transition heat-capacity data for 65OBC indicates approximate symmetry about the heat-capacity-peak temperatures (Figs. 3 and 4). Between successive heating and cooling runs of C_p versus T no thermal hysteresis was observable within the relative temperature resolution of the experiment (± 2 mK). If the SmA–hexatic-B transition of 65OBC has a latent heat, then a decrease in the average applied ac-heater power P_{ac} should result in an increase in the measured relative heat capacity C_p at the latent-heat temperature. In the presence of a latent heat (assumed to be at the heat-capacity-peak temperature T_p) a graph of P_{ac}/T_{ac} versus P_{ac} at T_p would show an increase in P_{ac}/T_{ac} as P_{ac} decreases. Here T_{ac} is the ac rms temperature-oscillation amplitude. Figure 10 shows P_{ac}/T_{ac} versus P_{ac} at the SmA–hexatic-B heat-capacity peak for 65OBC. Within the uncertainty of the data, P_{ac}/T_{ac} shows no consistent increase as P_{ac} decreases down to $T_{ac}=56$ μK rms. Therefore, the SmA–hexatic-B transition of 65OBC has no detectable latent heat within the uncertainty of the data.

The results of fitting the SmA–hexatic-B transition heat-capacity data for 65OBC (sample 2) to the power-law divergence $\Delta C_p = A^{\pm} \mid t \mid^{-\alpha^{\pm}}$ are $\alpha^- = \alpha^+ = 0.61 \pm 0.02$, $A^+/A^- = 0.84 \pm 0.03$, and $T_c = 67.290 \pm 0.003$ °C in the reduced temperature range $7.5\times10^{-5} \leq \mid t \mid \leq 1.5\times10^{-2}$. Previous results for 65OBC (sample 1)[12] were $\alpha^- = \alpha^+ = 0.64$, $A^+/A^- = 0.83$, and $T_c = 67.930 \pm 0.003$ °C in the reduced temperature range $2\times10^{-5} \leq \mid t \mid \leq 1.6\times10^{-2}$. The values of critical exponents α and amplitude ratios A^+/A^- are highly consistent for the two different samples of 65OBC. However, the value of T_c for the present data is lower by 0.64 °C. And the present data could only be fit to within 25 mK of T_c whereas the data for sample 1 came within 7 mK of T_c. Both the lower T_c and the smaller fitting range close to T_c (more heat-capacity-peak rounding) indicate that the present sample contained more impurities than sample 1. The present sample came from 65OBC prepared in a large quantity; the previous sample prepared on a small quantity. Prepared in large quantities, the purity of 65OBC is much harder to control, which is consistent with the above results. Rosenblatt and Ho,[15] using 65OBC from the large quantity preparation, also reported a similar T_c (67.370 °C) and fitting range limit ($\mid t \mid = 6\times10^{-5}$) close to T_c. Because both samples 1 and 2 gave consistent values for α, the impurities present in sample 2 do not change the nature of the SmA–hexatic-B transition in 65OBC.

For the 40.8-65OBC 10-90% mixture, the SmA–hexatic-B transition[9] showed thermal hysteresis. On successive heating ($T_{ph} = 67.323$ °C) and cooling ($T_{pc} = 67.308$ °C) trials the temperatures of peak heat capacity differ by 15 mK. By temperature-range-shrinking the data from 20 mK $\leq \mid T - T_c \mid \leq 8$ K to 100 mK $\leq \mid T - T_c \mid \leq 8$ K, the value of α and χ_ν^2 decreased and the value of α became asymptotic at 0.49 for a reasonable χ_ν^2 at $T_n = 100$ mK. Presumably for T_n too small, α becomes artifically large due to first-order behavior near T_c in agreement with the presence of thermal hysteresis. Therefore, the 40.8-65OBC 10-90% mixture system SmA–hexatic-B transition is weakly first order and was fitted to the power-law divergence $\Delta C_p = A^{\pm} \mid t \mid^{-\alpha^{\pm}}$ in the reduced temperature range $2.9\times10^{-4} \leq \mid t \mid \leq 2.3\times10^{-2}$ (100 mK $\leq \mid T - T_c \mid \leq 8$ K) which gave $\alpha = 0.49 \pm 0.02$, $A^+/A^- = 0.82 \pm 0.03$, and $T_c = 67.313$

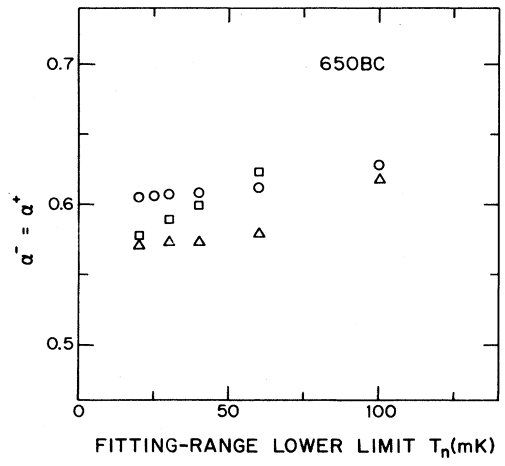

FIG. 9. $\alpha^- = \alpha^+$ vs temperature-fitting-range lower limit T_n (mK) for 65OBC. ○, temperature range T_n–5 K; □, two decade temperature range; △, one and one-half decade temperature range.

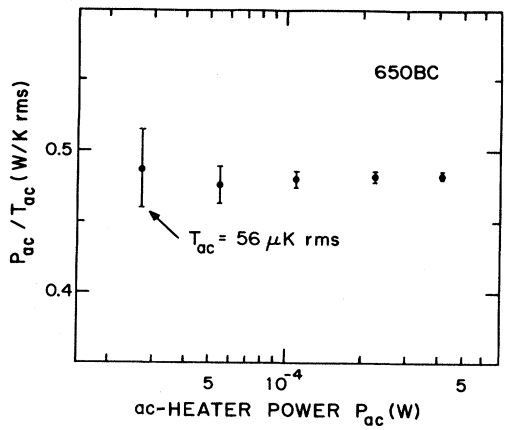

FIG. 10. P_{ac}/T_{ac} vs P_{ac} for 65OBC at the heat-capacity peak of the SmA–hexatic-B transition, where P_{ac} is the average ac-heater power and T_{ac} is the rms value of the temperature oscillation.

± 0.003 °C. The 4O.8-65OBC 30.5-69.5 % mixture system SmA-B transition is first order in nature. The heat-capacity-peak heights for heating and cooling differ by 11% and the temperatures of maximum heat-capacity heating ($T_{ph}=65.303$ °C) and cooling ($T_{pc}=65.141$ °C) differ by 162 mK, an indication of superheating and supercooling. Assuming that the T_c difference between samples 1 and 2 of undiluted 65OBC was due solely to impurities which had no affect on the nature of the SmA—hexatic-B transition, then the resulting change to first-order behavior from the impurity 4O.8 in 65OBC shows that different impurities affect the nature of the SmA—hexatic-B transition of 65OBC in different ways.

The large critical exponent $\alpha=0.6$ for 65OBC has also been confirmed in a detailed measurement of the $1-\alpha$ singularity of the in-plane position correlation of 65OBC.[24] The large value for the exponent α has ruled out the 3D XY model, the model that should apply to a phase transition with bond-orientation order as the order parameter. Also, the 2D four-state Potts model with $\alpha=\frac{2}{3}$ and $\beta=\frac{1}{12}$ is inconsistent with x-ray studies[10] and a measured value of the critical exponent $\beta=0.19$.[15] With x-ray measurements on free-standing films of bulk 65OBC, Pindak *et al.*[10] have shown that the SmA and hexatic-B phases contain local herringbone packing order. Precisely how herringbone order and the hexatic-B—E transition affect the SmA—hexatic-B transition is not known. For homologous series of *n*-alkyl-4′-*n*-alkoxybiphenyl-4-carboxylates, homologs with shorter alkyl chain lengths favor a SmA—hexatic-B—E phase-transition sequence.[25] Measurements are now in progress on such homologs for the purpose of testing how the alkyl chain length and the presence of the hexatic-B—E transition affect the nature of the SmA—hexatic-B transition.

Noting the presence of local herringbone order in the SmA and hexatic-B phases of 65OBC, Bruinsma and Aeppli[16] proposed a theory based on the coupling of bond-orientational and herringbone packing degrees of freedom in layered liquid crystals. The theory predicts that a continuous bond-orientational order transition in 3D can be driven first order by herringbone fluctuations and a tricritical point will separate the first- and second-order transition lines. Because the measured values of $\alpha=0.61$ and $\beta=0.19$ are close to the 3D Gaussian tricritical point values of $\alpha_t=0.5$ and $\beta_t=0.25$, the SmA—hexatic-B transition may be near a tricritical point. To test the Gaussian tricritical point hypothesis, first consider undiluted 65OBC. If the SmA—hexatic-B transition is near a Gaussian tricritical point, then $\alpha=0.61$ would be artifically high due to weakly first-order behavior near T_c. However, 65OBC has no thermal hysteresis and no latent heat within experimental error. In addition, Fig. 9 shows that α remains stable with temperature-range-shrinking, i.e., as T_n varies from 20 to 100 mK for a fitting range of $T_n \leq |T-T_c| \leq 5$ K, α varies from 0.60 to 0.63. If α were artificially high due to first-order behavior near T_c, then as the temperature-fitting range decreased, α would decrease. The lack of first-order behavior and the stability of $\alpha > \alpha_t$ with temperature-range-shrinking away from T_c contradict the Gaussian tricritical point hypothesis for pure 65OBC. Nevertheless, a tricritical point hypothesis could still be correct. A tricritical point with $\alpha \neq 0.5$, induced by fluctuations with symmetry of a cubic lattice, may be possible provided the fluctuation-induced and Gaussian tricritical points have different fixed points in renormalization group parameter space.[26]

The data for the SmA—hexatic-B transition of the 4O.8-65OBC mixture system does not violate a Gaussian tricritical point hypothesis. The transition shows weakly first-order behavior and temperature-range-shrinking from $T_n=20$ mK to 100 mK for a fitting range of $T_n \leq |T-T_c| \leq 5$ K indicates that α evolves from 0.59 to an asymptotic value of 0.49 ± 0.02, a value consistent with $\alpha_t=0.5$. Studies on the mixture system should provide further insight into the nature of SmA—hexatic-B transition.

Heat-capacity measurements[27] on the liquid crystal *n*-nonyl-4′-*n*-pentyloxybiphenyl-4-thiocarboxylate (95SBC) have shown the SmA—hexatic-B transition to be first order. This is consistent with x-ray structure measurements[24] with show an abrupt change in the in-plane correlation length with no pretransitional behavior. In the hexatic-B phase of 95SBC, $\xi_{11} \sim 300$ Å compared to $\xi_{11} \sim 100$ Å for 65OBC. Therefore, the coupling of in-plane positional order with bond-orientational order may drive the SmA—hexatic-B transition to 95SBC first order. The liquid crystal 4O.8 has crystalline-B phase with long-range in-plane and interplane couplings. The addition of 4O.8 to 65OBC seems to increase the in-plane and interplane coupling of the hexatic-B phase for 65OBC and drive the SmA—hexatic-B transition of 95SBC first order. denced by the results of 10% and 30.5% mixtures of 4O.8 in 65OBC. Finally, a recent pressure study of 65OBC by Cladis and Goodby[28] revealed that the hexatic-B phase collapses to the crystalline-B phase for pressures greater than 1.5 kbar, which suggests that in-plane and/or interplane correlations play a role as to the nature of the liquid-crystal B phase as well as the SmA—B transition. Consequently, any theory which neglects the effect of the in-plane correlation length may be incomplete as to explain the nature of the SmA—hexatic-B transition in 65OBC. In particular, the neglect of in-plane correlation length may be the reason that the measured exponents α and β differ from Gaussian tricritical values. Further experiments on 65OBC-95SBC mixtures and/or 65OBC under pressure should cast some light on the role played by in-plane correlation length.

ACKNOWLEDGMENTS

It is a pleasure to thank P. C. Hohenberg, D. R. Nelson, P. M. Horn, J. W. Halley, and R. Bruinsma for helpful discussions, W. Zimmermann for allowing us to use his vacuum evaporating system, and S. C. Lien for his assistance with experimental measurements. This work was partially supported by the U. S. Department of Energy under Contract No. DE-AC02-79ER10461 and by the University of Minnesota Computer Center. One of us (J.M.V.) acknowledges the support from the National Science Foundation, Solid State Chemistry, Program Grant No. DMR-82-04219.

[1]A. M. Levelut, J. Doucet, and M. Lambert, J. Phys. (Paris) 35, 773 (1974).

[2]A. De Vries, A. Ekachai, and N. Spielberg, J. Phys. (Paris), Colloq. 40, C3-147 (1979); A. J. Leadbetter, J. Frost, J. P. Gaughan, and M. A. Mazid, *ibid.* 40, C3-185 (1979); J. Doucet, A. M. Levelut, and M. Lambert, Ann. Phys. (N.Y.) 3, 157 (1978).

[3]A. J. Leadbetter, M. A. Mazid, B. A. Kelley, J. Goodby, and G. W. Gray, Phys. Rev. Lett. 43, 630 (1979).

[4]D. E. Moncton and R. Pindak, Phys. Rev. Lett. 43, 701 (1979); D. E. Moncton and R. Pindak, *Ordering in Two Dimensions,* edited by S. K. Sinha (North-Holland, New York, 1980).

[5]P. S. Pershan, G. Aeppli, J. D. Litster, and R. J. Birgeneau, Mol. Cryst. Liq. Cryst. 67, 205 (1981).

[6]A. J. Leadbetter, J. C. Frost, and M. A. Mazid, J. Phys. (Paris) Lett. 40, L-325 (1978).

[7]R. J. Birgeneau and J. D. Litster, J. Phys. (Paris) Lett. 39, L-399 (1978).

[8]B. I. Halperin and D. R. Nelson, Phys. Rev. Lett. 41, 121 (1978); D. R. Nelson and B. I. Halperin, Phys. Rev. B 19, 2457 (1979).

[9]J. W. Goodby and R. Pindak, Mol. Cryst. Liq. Cryst. 75, 233 (1981).

[10]R. Pindak, D. E. Moncton, S. C. Davey, and J. W. Goodby, Phys. Rev. Lett. 46, 1135 (1981).

[11]A. M. Levelut, J. Phys. (Paris) Colloq. 37, C3-51 (1976).

[12]C. C. Huang, J. M. Viner, R. Pindak, and J. W. Goodby, Phys. Rev. Lett. 46, 1289 (1981). The 4O.8-65OBC mixture systems were prepared from the same 65OBC as used in Ref. 12. The 65OBC used in the present paper came from a different preparation. See the text for additional details.

[13]R. Pindak, W. O. Sprenger, D. J. Bishop, D. D. Osheroff, and J. W. Goodby, Phys. Rev. Lett. 48, 173 (1982).

[14]R. Pindak, D. J. Bishop, and W. O. Sprenger, Phys. Rev. Lett. 44, 1461 (1980).

[15]C. Rosenblatt and J. T. Ho, Phys. Rev. A 26, 2293 (1982).

[16]R. Bruinsma and G. Aeppli, Phys. Rev. Lett. 48, 1625 (1982).

[17]P. Sullivan and G. Seidel, Phys. Rev. 173, 679 (1968).

[18]J. E. Smaardyk and J. M. Mochel, Rev. Sci. Instrum. 49, 988 (1978); J. D. Le Grange and J. M. Mochel, Phys. Rev. A 23, 3215 (1981).

[19]C. A. Schantz and D. L. Johnson, Phys. Rev. A 17, 1504 (1978).

[20]G. B. Kasting, K. J. Lushington, and C. W. Garland, Phys. Rev. B 22, 321 (1980).

[21]P. R. Bevington, *Data Reduction and Error Analysis for the Physical Sciences* (McGraw-Hill, New York, 1969).

[22]F. L. Lederman, M. B. Salamon, and L. W. Shacklette, Phys. Rev. B 9, 2981 (1974); F. L. Lederman, Ph.D. thesis, University of Illinois at Urbana-Champaign, 1980 (unpublished).

[23]A. Ralston, *A First Course in Numerical Analysis* (McGraw-Hill, New York, 1965), Chap. 6.

[24]S. C. Davey, E. Fontes, J. W. Goodby, R. Pindak, and D. E. Moncton (unpublished).

[25]J. W. Goodby and G. W. Gray, J. Phys. (Paris), Colloq. 37, C3-17 (1976).

[26]A. Aharony (private communication).

[27]C. C. Huang (unpublished).

[28]P. E. Cladis and J. W. Goodby, Mol. Cryst. Liq. Cryst. Lett. 72, 307 (1982).